

1 **Investigations on the hypocholesterolaemic activity of LILPKHSDAD**
2 **and LTFPGSAED, two peptides from lupin β -conglutin: focus on**
3 **LDLR and PCSK9 pathways**

4
5 *Chiara Zanoni, Gilda Aiello, Anna Arnoldi,* Carmen Lammi*

6 Department of Pharmaceutical Sciences, University of Milan, 20133 Milan, Italy

7
8 *Corresponding author: Anna Arnoldi, Department of Pharmaceutical Sciences, University of
9 Milan, via Mangiagalli 25, 20133 Milan, Italy. Tel +390250319372, anna.arnoldi@unimi.it

10
11 **ABSTRACT.**

12 **P5** (LILPKHSDAD) and **P7** (LTFPGSAED) are two peptides from lupin protein that are absorbed in
13 Caco-2 cells. Recent *in silico* docking studies had suggested that they could potentially function as
14 inhibitors of 3-hydroxy-3-methylglutaryl CoA reductase (HMGCoAR) activity. This paper confirms
15 that both peptides inhibit *in vitro* the HMGCoAR functionality and it reports the characterisation of
16 the molecular mechanism through which they modulate the cholesterol metabolism in HepG2 cells.
17 Through the inhibition of HMGCoAR activity, **P5** and **P7** are able to improve the LDLR protein
18 levels leading to a better ability of HepG2 cells to uptake extracellular LDL molecules with a final
19 hypocholesterolaemic effects. The modulation of PCSK9 intracellular processing was also evaluated:
20 only **P5** was able to decrease the PCSK9 and HNF1-alpha protein levels leading to a decrease of
21 mature PCSK9 secretion by HepG2 cells.

22
23 **Keywords:** bioactive peptides, functional foods, LDL receptor, PCSK9, plant protein.

24
25 **Abbreviations:** AMPK, adenosine monophosphate-activated protein kinase; DMEM, Dulbecco's
26 modified Eagle's medium; FBS, foetal bovine serum; HMGCoAR, 3-hydroxy-3-methylglutaryl CoA
27 reductase; HNF1-alpha, hepatocyte nuclear factor 1-alpha; LDL, low density lipoprotein; LDLR,
28 LDL receptor; PCSK9, proprotein convertase subtilisin/kexin type 9; SREBP2, sterol regulatory
29 element binding protein 2.

30

31

32 1. Introduction

33 Lupin protein and peptides provide useful health benefits (Arnoldi, Boschin, Zanoni, & Lammi, 2015;
34 Duranti, Consonni, Magni, Sessa, & Scarafoni, 2008), particularly in the area of cholesterol reduction
35 (Bähr, Fechner, Kiehntopf, & Jahreis, 2015; Sirtori, Triolo, Bosisio, Bondioli, Calabresi, De Vergori,
36 et al., 2012), hypertension control (Arnoldi, Boschin, Zanoni, & Lammi, 2015), and hyperglycaemia
37 prevention (Duranti et al., 2008).

38 Convinced that these activities should be ascribed to specific peptides initially encrypted in the
39 protein sequences and released by digestion, in the last few years, we have dedicated much effort to
40 investigate the biological activity and the bioavailability of lupin peptides, with particular focus on
41 cholesterol reduction. Working on human hepatic HepG2 cells, it was possible to demonstrate that
42 tryptic and peptic hydrolysates from a total lupin protein extract are able to interfere with the
43 HMGCoAR activity, up-regulating the LDL receptor (LDLR) and sterol regulatory element binding
44 protein 2 (SREBP2) proteins via the activation of phosphoinositide 3-kinase (PI3K), protein kinase
45 B (Akt), and glycogen synthase kinase-3 β (GSK3 β) pathways and increasing the LDL-uptake of
46 HepG2 cells (Lammi, Zanoni, Scigliuolo, D'Amato, & Arnoldi, 2014). As indicated by chip-HPLC-
47 ESI-MS/MS analysis, the composition of both hydrolysates was very complex, with a prevalence of
48 peptides deriving from β -conglutin, a major storage protein belonging to the vicilin-like family
49 (Duranti et al., 2008).

50 In order to sort out potentially bioavailable peptides among those detected, a model of the intestine
51 based on differentiated human intestinal Caco-2 cells was used (Ferruzza, Rossi, Scarino, & Sambuy,
52 2012; Sambuy, De Angelis, Ranaldi, Scarino, Stammati, & Zucco, 2005). The hydrolysates were
53 added in the apical chamber of a two-chambers system and after 4 h the basolateral solutions were
54 collected and analysed by HPLC-Chip-MS/MS. This permitted the identification of eleven tryptic
55 and eight peptic peptides. Interestingly, a specific assay showed that the basolateral samples still kept
56 up the capacity to inhibit the activity of HMGCoAR (Lammi, Aiello, Vistoli, Zanoni, Arnoldi,
57 Sambuy, et al., 2016).

58 A further experiment, conducted in a co-culture system in which Caco2 cells and HepG2 cells were
59 combined, showed that the basolateral solutions from the peptic and tryptic hydrolysate treatments
60 are still bioactive on HepG2 cells, with an intensity that was even improved by the crosstalk between
61 the two cell systems in co-culture (Lammi, Zanoni, Ferruzza, Ranaldi, Sambuy, & Arnoldi, 2016).
62 All these evidences suggest that the basolateral samples should contain very active peptides. In order
63 to identify the most active ones, it was decided to perform *in silico* docking simulations with the
64 catalytic site of HMGCoAR: two peptides LILPKHSDAD (**P5**) and LTFPGSAED (**P7**), derived from
65 β -conglutin, appeared to be potentially the major amino acid sequences responsible of the observed

66 activity, because they bind very efficiently to the catalytic site of this enzyme showing the best
67 normalised Plp95, APBS and MLP score values in the docking simulations (Lammi, et al., 2016).
68 Based on these considerations, this work had two main objectives: 1) the experimental confirmation
69 that indeed **P5** and **P7** are able to inhibit the HMGCoAR activity as suggested by the preceding *in*
70 *silico* simulations; 2) the detailed investigation of the mechanism of action through which these
71 peptides exert their hypocholesterolaemic effects in HepG2 cells at molecular and functional levels.

72

74 **2. Materials and methods**

75 **2.1 Materials**

76 Dulbecco's modified Eagle's medium (DMEM), L-glutamine, foetal bovine serum (FBS), phosphate
77 buffered saline (PBS), penicillin/streptomycin, chemiluminescent reagent, and 96-well plates were
78 purchased from Euroclone (Milan, Italy). Bovine serum albumin (BSA), RIPA buffer, and the
79 antibody against β -actin were bought from Sigma-Aldrich (St. Louis, MO, USA). The antibody
80 against HMGCoAR was bought from Abcam (Cambridge, UK). The antibody against phospho-
81 HMGCoAR (Ser872) was purchased from Bioss Antibodies (Woburn, MA, USA). The antibody
82 against proprotein convertase subtilisin/kexin type 9 (PCSK9) and hepatocyte nuclear factor 1-alpha
83 (HNF1-alpha) were bought from GeneTex (Irvine, CA, USA). Phenylmethanesulfonyl fluoride
84 (PMSF), Na-orthovanadate inhibitors, and the antibodies against rabbit Ig-horseradish peroxidase
85 (HRP), mouse Ig-HRP, and SREBP-2 were purchased from Santa Cruz Biotechnology Inc. (Santa
86 Cruz, CA, USA). The antibodies against the LDLR and the phospho-AMPK (Thr172) were bought
87 from Pierce (Rockford, IL, USA). The inhibitor cocktail Complete Midi from Roche (Basel, Swiss).
88 Mini protean TGX pre-cast gel 7.5% and Mini nitrocellulose Transfer Packs were purchased from
89 BioRad (Hercules, CA, USA). The Human Proprotein Convertase 9 Immunoassay (Quantikine
90 ELISA) was bought from R&D System (Minneapolis, MN, USA). Synthetic peptides **P5** and **P7** were
91 synthesized by the company PRIMM (Milan, Italy) at >95% purity.

92

93 **2.2 Cell culture conditions**

94 HepG2 cell line was bought from ATCC (HB-8065, ATCC from LGC Standards, Milan, Italy) and
95 was cultured in DMEM high glucose with stable L-glutamine, supplemented with 10% FBS, 100
96 U/mL penicillin, 100 μ g/mL streptomycin (complete growth medium) with incubation at 37 °C under
97 5% CO₂ atmosphere. HepG2 cells were used for no more than 20 passages after thawing, because the
98 increase in number of passages may change the cell characteristics and impair assay results.

99

100 **2.3 HMGC_oAR activity assay**

101 The assay buffer, NADPH, substrate solution, and HMGC_oAR were provided in the HMGC_oAR
102 Assay Kit (Sigma). The experiments were carried out following the manufacturer's instructions at 37
103 °C. In particular, each reaction (200 µL) was prepared adding the reagents in the following order: 1
104 X assay buffer, a concentration range of **P5** and **P7** from 10⁻⁵ to 10⁻³ M or vehicle (C), the NADPH
105 (4 µL), the substrate solution (12 µL), and finally the HMGC_oAR (catalytic domain) (2 µL).
106 Subsequently, the samples were mixed and the absorbance at 340 nm read by a microplate reader
107 Synergy H1 from Biotek at time 0 and 10 min. The HMGC_oAR-dependent oxidation of NADPH and
108 the inhibition properties of lupin peptides were measured by absorbance reduction, which is directly
109 proportional to enzyme activity.

110

111 **2.4 Western blot analysis**

112 A total of 1.5 x 10⁵ HepG2 cells/well (24-well plate) were treated with 50 and 100 µM of **P5** and 10
113 and 50 µM of **P7** for 24 h. After each treatment, cells were scraped in 40 µL ice-cold lysis buffer
114 [RIPA buffer + inhibitor cocktail + 1:100 PMSF + 1:100 Na-orthovanadate] and transferred in an ice-
115 cold microcentrifuge tube. After centrifugation at 16,060 g for 15 min at 4 °C, the supernatant was
116 recovered and transferred into a new ice-cold tube. Total proteins were quantified by Bradford method
117 and 50 µg of total proteins loaded on a pre-cast 7.5% Sodium Dodecyl Sulphate - Polyacrylamide
118 (SDS-PAGE) gel at 130 V for 45 min. Subsequently, the gel was pre-equilibrated with 0.04% SDS
119 in H₂O for 15 min at room temperature (RT) and transferred to a nitrocellulose membrane (Mini
120 nitrocellulose Transfer Packs,) using a Trans-Blot Turbo at 1.3 A, 25 V for 7 min. Target proteins,
121 on milk blocked membrane, were detected by primary antibodies as follows: rabbit anti-SREBP2,
122 rabbit anti-LDLR, anti-HMGC_oAR, anti-phospho AMPK (Thr172), anti-phospho HMGC_oAR
123 (Ser872), anti-HNF1 alpha, anti-PCSK9, and anti-β-actin. Secondary antibodies conjugated with
124 HRP and a chemiluminescent reagent were used to visualize target proteins and their signal was
125 quantified using the Image Lab Software (Biorad). The internal control β-actin was used to normalise
126 loading variations.

127

128 **2.5 Assay for evaluation of fluorescent LDL uptake by HepG2 cells**

129 A total of 3 x 10⁴ HepG2 cells/well were seeded in 96-well plates and kept in complete growth
130 medium for 2 d before treatment. On the third day, cells were treated with 10 and 50 µM of **P5** and
131 **P7**, respectively, or vehicle (H₂O) for 24 h. At the end of the treatment period, the culture medium
132 was replaced with 75 µL/well LDL-DyLight™ 550 working solution. The cells were additionally

133 incubated for 2 h at 37 °C and then the culture medium was aspirated and replaced with PBS (100
134 µL/well). The degree of LDL uptake was measured using the Synergy H1 fluorescent plate reader
135 from Biotek (excitation and emission wavelengths 540 and 570 nm, respectively).

136

137 **2.6 Quantification of PCSK9 excreted by HepG2 cells through ELISA**

138 The supernatants collected from HepG2 cells were centrifuged at 600 g for 10 min at 4 °C. They were
139 recovered and diluted to the ratio 1:10 with DMEM in a new ice-cold tube. PCSK9 was quantified
140 by ELISA (R&D System, Minneapolis, MN, USA). Briefly, the experiments were carried out at 37
141 °C, following the manufacturer's instructions. Before starting the assay, human PCSK9 standards
142 (20.0, 10.0, 5.0, 2.5, 1.25, and 0.625 ng/mL) were prepared from the stock PCSK9 standard solution
143 (40 ng/mL) with serial dilutions (for building the standard curve) and meanwhile 100 µL of the Assay
144 Diluent RD1-9 (provided into the kit) were added to each wells. Afterward, standards and samples
145 (50 µL) were pipetted into the wells and the ELISA plate was allowed to incubate for 2 h at RT.
146 Subsequently, wells were washed 4 times with Wash Buffer, and 200 µL of human PCSK9-Conjugate
147 (HRP-labelled anti-PCSK9) was added to each wells for a 2 h incubation at RT. Following aspiration,
148 well was washed 4 times with Wash Buffer provided by the kit. After the last wash, 200 µL of
149 Substrate Solution were added to the wells and allowed to incubate for 30 min at RT. The reaction
150 was stopped with 50 µL of Stop Solution (2 N sulfuric acid) and the absorbance at 450 nm was
151 measured using Synergy H1 (Biotek, Bad Friedrichshall, Germany). The lower limit of detection was
152 0.096 ng/mL.

153

154 **2.7 Statistically Analysis**

155 Statistical analyses were carried out by One-way ANOVA (Graphpad Prism 6) followed by Dunnett's
156 test. Values were expressed as means ± sem; P-values < 0.05 were considered to be significant.

157

158

159 **3. Results**

160 **3.1. Inhibition of the catalytic activity of HMGCoAR**

161 In order to confirm the *in silico* prediction according to which **P5** and **P7** might be potential inhibitors
162 of the catalytic activity of HMGCoAR (Lammi, et al., 2016), an *in vitro* assay was performed using
163 the purified catalytic domain of this enzyme. Peptide concentrations ranging from 10⁻⁵ to 10⁻³ M were
164 tested. Each peptide inhibited HMGCoAR in a dose-dependent manner (Figure 1). The IC₅₀ value of
165 **P5** was equal to 147.2 ± 1.34 µM and that of **P7** was equal to 68.4 ± 1.53 µM. Based on these results,
166 **P7** appeared to be a more potent inhibitor of the HMGCoAR catalytic activity.

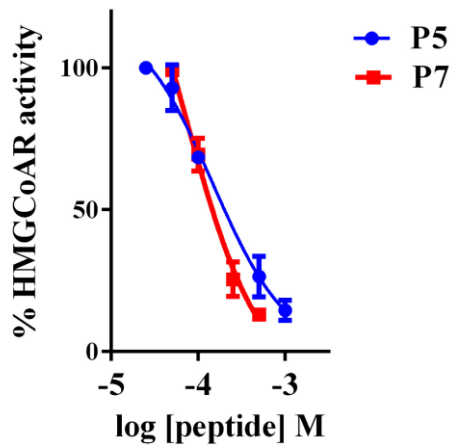
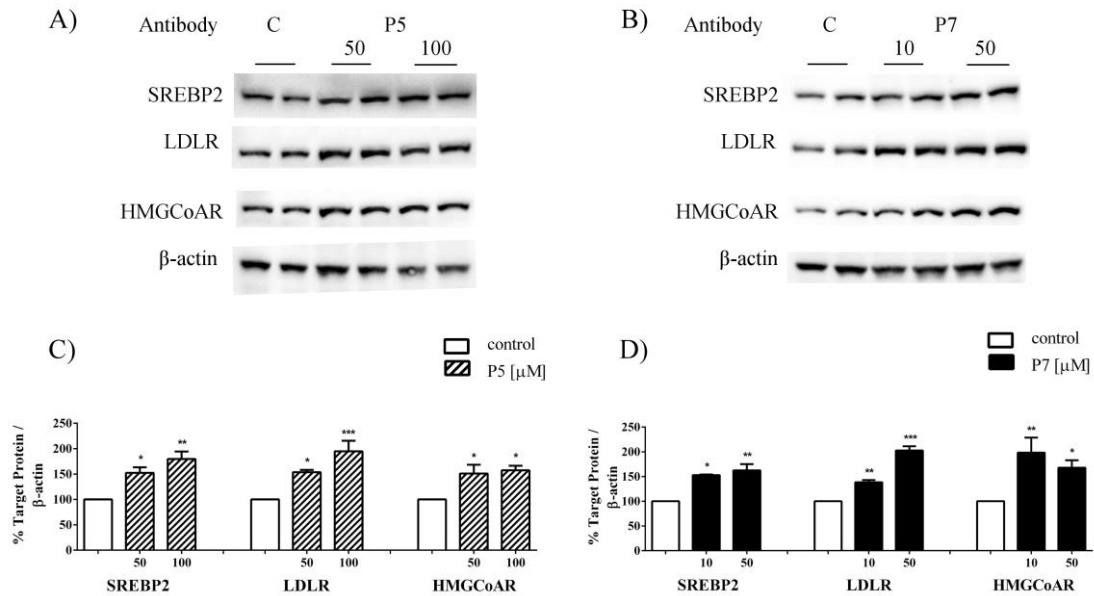


Figure 1. Concentration-response curves of the inhibitory effect of P5 and P7 on HMGCoAR activity.

The HMGCoAR, physiologically, catalyzes the four-electron reduction of HMGCoA to coenzyme A (CoA) and mevalonate ($\text{HMGCoA} + 2\text{NADPH} + 2\text{H}^+ > \text{mevalonate} + 2\text{NADP}^+ + \text{CoA-SH}$). In this assay, the decrease in absorbance at 340 nm, which represents the oxidation of NADPH by the catalytic subunit of HMGCoAR in the presence of the substrate HMGCoA, was measured spectrophotometrically for each peptide dose tested. IC₅₀ value for P5 is equal to $147.2 \pm 1.34 \mu\text{M}$, for P7 is equal to $68.4 \pm 1.53 \mu\text{M}$. Each point represents the average \pm SEM of three experiments in duplicate.

3.2 Activation of the LDLR pathway

HepG2 cells were treated with **P5** (50 and 100 μM) and **P7** (10 and 50 μM) and each sample was investigated with immunoblotting experiments. Figure 2A,C shows that the treatment with **P5** induced an up-regulation of the protein level of N-terminal fragment of the SREBP2 (mature form with a molecular weight of 68 kDa) by $52.3 \pm 18\%$ ($p < 0.05$) and $79.6 \pm 29.5\%$ ($p < 0.001$) at 50 μM and 100 μM , respectively, *versus* the control. As a consequence, up-regulations of the LDLR and HMGCoAR protein levels were also observed. In particular, after treatment with **P5** at 50 μM and 100 μM (Figure 2A,C), the LDLR protein level was increased by $53.5 \pm 9.4\%$ ($p < 0.05$) and $94.8 \pm 46.3\%$, ($p < 0.0001$) respectively, *versus* the control, whereas the HMGCoAR protein level was augmented by $51.2 \pm 29.8\%$ ($p < 0.05$) and $57.5 \pm 15.2\%$ ($p < 0.05$), respectively, *versus* the control. Figure 2 B,D shows, instead, the variations induced by treatments with 10 μM and 50 μM **P7** *versus* the control. The SREBP2 protein level was increased by $52.8 \pm 1.69\%$ ($p < 0.05$) and $62.46 \pm 28.18\%$ ($p < 0.001$) respectively; the LDLR protein level was augmented by $38.4 \pm 7.9\%$ ($p < 0.001$) and $102.7 \pm 16.8\%$ ($p < 0.0001$), respectively; whereas the HMGCoAR protein level was enhanced by $98.3 \pm 52.6\%$ ($p < 0.001$) and $67.8 \pm 33.7\%$ ($p < 0.05$), respectively, *versus* the control.



191

192 **Figure 2. Effects of P5 and P7 on SREBP2, LDLR, and HMGCoAR protein levels.** HepG2 cells (1.5×10^5) were treated with **P5** (50 and 100 μM) (A-C) and **P7** (10 and 50 μM) (B-D) for 24 h. SREBP2, LDLR, HMGCoAR, and β -actin immunoblotting signals were detected using specific anti-SREBP2, anti-LDLR, anti-HMGCoAR, and anti- β -actin primary antibodies, respectively. Each protein signal was quantified by ImageLab software (Biorad) and normalised with β -actin signals. Bars represent averages \pm SEM of six independent experiments (two duplicates per sample). (*) $p < 0.05$, (**) $p < 0.001$, and (***) $p < 0.0001$ versus control (C).

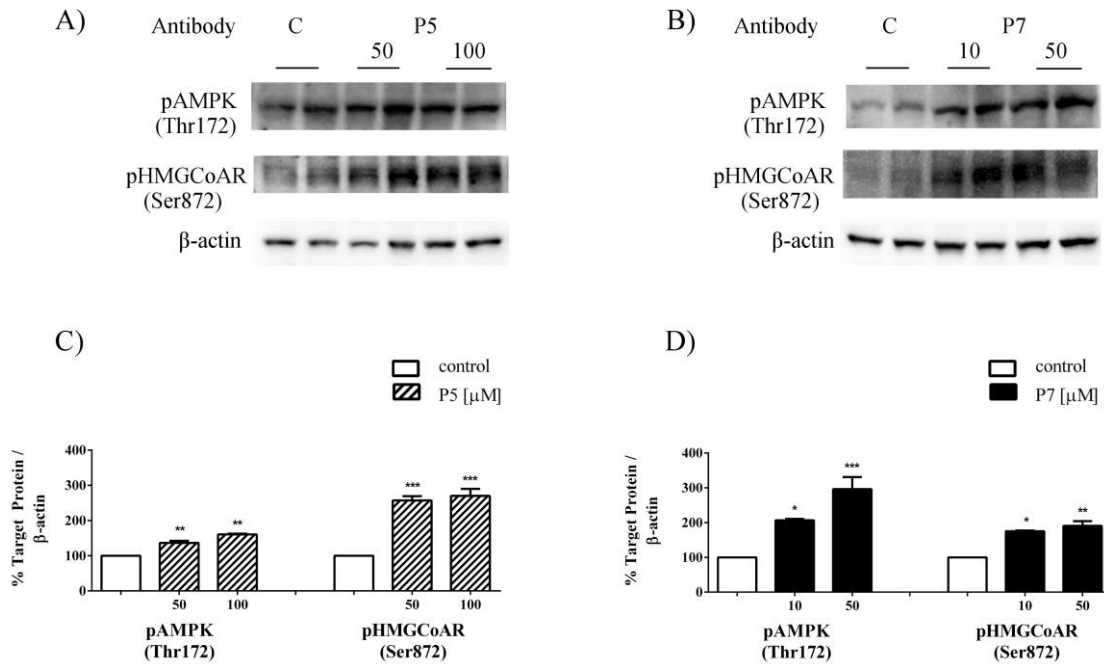
199

200

201 3.3 The inactivation of HMGCoAR depends on activation of the AMPK pathway

202 Suitable immunoblotting experiments were performed in order to evaluate the effect of the treatment with the same peptides on AMPK activation and HMGCoAR inactivation (AMPK substrate). The lysates from treated and untreated HepG2 cells were therefore analysed using specific antibodies for AMPK phosphorylated at threonine 172 (Figure 3A) and for HMGCoAR phosphorylated at serine 872 (AMPK phosphorylation site) (Figure 3B). Figure 3C shows that treatment with **P5** significantly increased AMPK phosphorylation by $36.5 \pm 8.3\%$ (50 μM , $p < 0.001$) and by $60.5 \pm 2.8\%$ (100 μM , $p < 0.001$), whereas the treatment with **P7** significantly increased the AMPK phosphorylation by $106.6 \pm 6.42\%$ (10 μM , $p < 0.05$) and $196.4 \pm 69.3\%$ (50 μM , $p < 0.0001$) versus the control. As a consequence of the AMPK activation, the phosphorylation levels of HMGCoAR were also increased (Figure 3D): after treatment with **P5** by $157.0 \pm 21.1\%$ (50 μM , $p < 0.0001$) and $169.9 \pm 35.0\%$ (100 μM , $p < 0.0001$), whereas after treatment with **P7** by $75.3 \pm 2.9\%$ (10 μM , $p < 0.05$) and $90.4 \pm 19.2\%$ (50 μM , $p < 0.001$) versus the control.

213



214

215

216

217

218

219

220

221

222

223

224

225

226

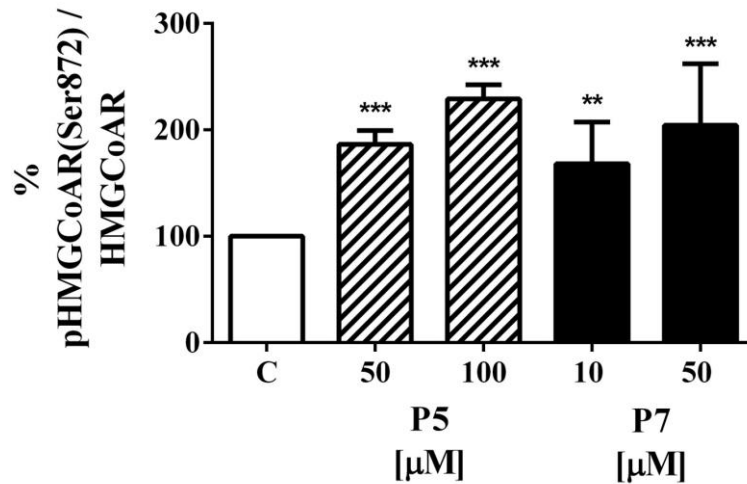
227

228

229

Figure 3. Effect of P5 and P7 on AMPK activation and HMGCoAR inactivation. HepG2 cells (1.5×10^5) were treated with **P5** (50 and 100 μ M) (A-C) and **P7** (10 and 50 μ M) (B-D) for 24 h. The phosphorylation levels of AMPK (Thr172) and HMGCoAR (Ser872) and β -actin immunoblotting signals were detected using specific anti-phospho AMPK (Thr172), anti-phospho HMGCoAR (Ser872), and anti- β -actin primary antibodies, respectively. Each protein signal was quantified by ImageLab software (Biorad) and normalised with β -actin signals. Bars represent averages \pm SEM of six independent experiments (two duplicates per sample). (*) $p < 0.05$, (**) $p < 0.001$, and (***) $p < 0.0001$ versus control (C).

Figure 4 clearly shows that the treatments with **P5** and **P7** led to an elevation of the p-HMGCoAR/HMGCoAR protein ratio indicating a diminished enzyme activity. In particular, the ratio phospho (p)-HMGCoAR/HMGCoAR protein increased by $86.2 \pm 16.2\%$ (50 μ M, $p < 0.0001$) and $129.1 \pm 13.4\%$ (100 μ M, $p < 0.0001$) versus the control after treatment with **P5**, and by $68.2 \pm 39.1\%$ (10 μ M, $p < 0.001$) and $104.2 \pm 57.8\%$ (50 μ M, $p < 0.0001$) after treatment with **P7**.



230

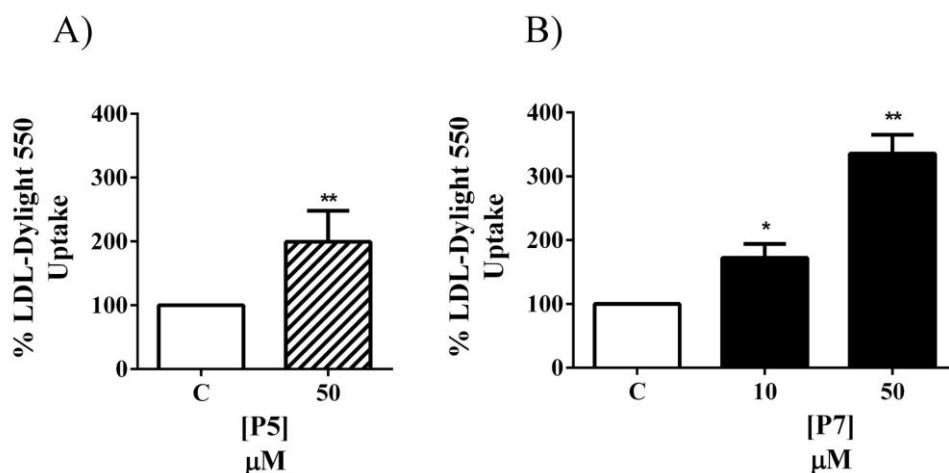
231 **Figure 4. Ratios between p-HMGCoAR (Ser872) and HMGCoAR protein levels.** Bars represent the
 232 ratios between p-HMGCoAR (Ser872) and HMGCoAR, each normalised with β -actin signals, after **P5** (50
 233 and 100 μ M) and **P7** (10 and 50 μ M) treatments. Bars represent averages \pm SEM of six independent
 234 experiments (two duplicates per sample). (**) $p < 0.001$, and (***) $p < 0.0001$ versus control (C).

235

236

237 **3.4 Modulation of the LDL-uptake in HepG2 cells**

238 The change of the functional capability of HepG2 cells to uptake extracellular LDL after the
 239 treatments with the peptides was investigated by performing fluorescent-LDL uptake experiments.
 240 As shown in Figure 5, each peptide increased the LDL-uptake in a statistically significant way *versus*
 241 the control. In fact, after treatments with 10 μ M and 50 μ M **P7**, the LDL-uptake was increased by
 242 $72.4 \pm 21.6\%$ ($p < 0.05$) and $235.9 \pm 29.2\%$ ($p < 0.001$), respectively (Figure 5B), whereas the
 243 treatments with **P5** at a concentration of 50 μ M led to an increase of the LDL-uptake by $99.5 \pm$
 244 48.51% ($p < 0.001$) (Figure 5A). At the concentration of 10 μ M, **P5** led to a $66 \pm 21.4\%$ ($p < 0.001$)
 245 increase as reported in another publication (Lammi, Zanoni, Aiello, Arnoldi, & Grazioso, 2016).

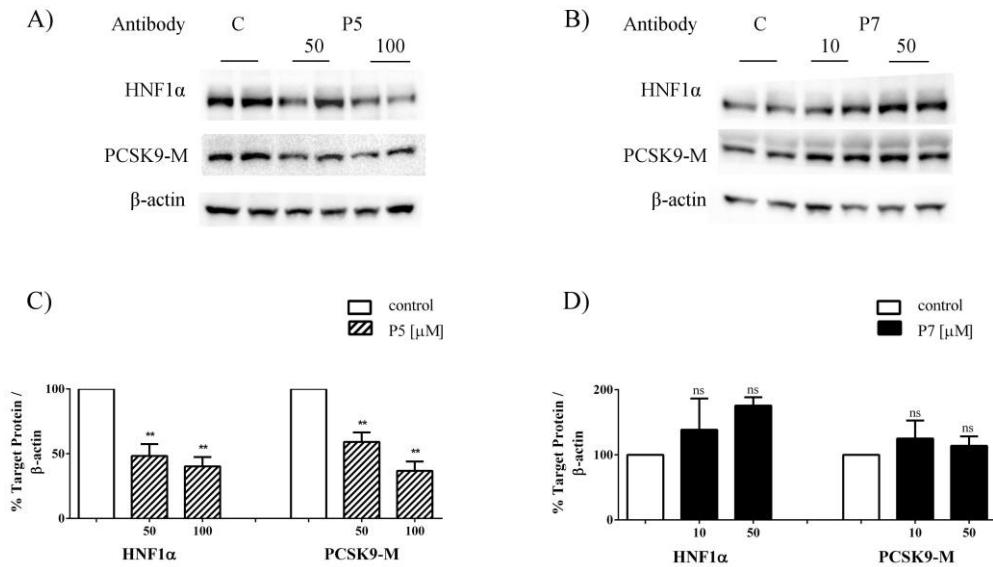


246

247 **Figure 5. Fluorescent LDL-uptake assay after treatments of HepG2 with P5 and P7.** Cells (3×10^4)
 248 were treated with **P5** (50 μM) (A) and **P7** (10 and 50 μM) (B) for 24 h. LDL-Dylight 549 (10 $\mu\text{g}/\text{mL}$) was
 249 incubated for an additional 2 h. Excess LDL-Dylight 549 was removed and cells were washed two times with
 250 PBS. Specific fluorescent LDL-uptake signal was analysed by Synergy H1 (Biotek). Data points represent
 251 averages \pm SEM of three independent experiments in triplicate. (*) $p < 0.05$ and (**) $p < 0.001$ versus control
 252 (C).
 253

254 3.5 Modulation of the PCSK9 and HNF1-alpha protein levels

255 Further experiments were conducted with the objective of evaluating the effects of the treatments of
 256 HepG2 cells with **P5** (50 and 100 μM) and **P7** (10 and 50 μM) on the modulation of PCSK9. Mature
 257 PCSK9 (molecular weight ~ 62 kDa, PCSK9-M) was detected by immunoblotting using a specific
 258 antibody. Whereas the treatment with **P7** did not produce any statistically significant change (Figure
 259 6D), the treatment with **P5** (Figure 6A,B) induced a $40.8 \pm 12.6\%$ ($p < 0.001$) increase in PCSK9-M
 260 protein level at a 50 μM concentration and a $63.3 \pm 10.2\%$ ($p < 0.001$) augmentation at 100 μM versus
 261 the untreated sample (Figure 6C). In parallel, the same peptides had different effects on HNF1-alpha
 262 protein levels (Figure 6A,B), since **P5** decreased HNF-1 alpha level by $51.7 \pm 18.4\%$ ($p < 0.001$) at 50
 263 μM and by $59.8 \pm 14.3\%$ ($p < 0.001$) at 100 μM , versus the untreated sample (Figure 6C), whereas **P7**
 264 was essentially inactive (Fig 6D).
 265



266

267 **Figure 6. Effects of P5 and P7 on PCSK9 and HNF1-alpha protein levels.** HepG2 cells (1.5×10^5) were
 268 treated **P5** (50 μ M) (A-C) and **P7** (10 and 50 μ M) (B-D) for 24 h. PCSK9, HNF1-alpha and β -actin
 269 immunoblotting signals were detected using specific anti-PCSK9, anti-HNF1-alpha and anti- β -actin primary
 270 antibodies, respectively. PCSK9-M represents the cleaved mature form of PCSK9. PCSK9-M and HNF1-
 271 alpha signals were quantified by ImageLab software (Biorad) and normalised with β -actin signals. Bars
 272 represent averages \pm SEM of six independent experiments (two duplicates per sample). (**) $p < 0.001$ versus
 273 control (C).
 274

275 3.6. P5 reduces the secretion of PCSK9-M by HepG2 cells

276 It was then decided to evaluate whether **P5** was also able to modulate the secretion of PCSK9-M by
 277 HepG2 cells. For this scope, the same cells were treated with **P5** (50 and 100 μ M) for 24 h. On the
 278 second day, the cell culture medium was collected and secreted PCSK9-M measured using a specific
 279 ELISA kit. The data of Table 1 clearly indicate that **P5** induced a small but significant reduction of
 280 the secretion of PCSK9-M *versus* the untreated samples: at 50 μ M concentration secreted PCSK9
 281 was lessened by 19.7% (63.7 ± 4.0 ng/mL, $p < 0.05$) and at 100 μ M concentration by 27.3% ($57.7 \pm$
 282 $13.$ ng/mL, $p < .001$) *versus* control (79.4 ± 1.0 ng/mL). **P7** was not investigated here, since it had
 283 been shown to be inactive during modulation of PCSK9 and HNF1-alpha protein levels.
 284

Table 1 – Effect of **P5** and **P7** peptides on secreted PCSK9 media levels in HepG2 cells

Parameter	C	P 5	
		50 μ M	100 μ M

Secreted PCSK9 levels (ng/mL)	79.4± 1.0	63.7 ± 4.0 *	57.7 ± 13.4 **
----------------------------------	-----------	--------------	----------------

* $P < 0.05$ vs untreated sample (C); ** $P < 0.001$ vs untreated sample (C)

285

286

287 4. Discussion

288 4.1 Modulation of cholesterol homeostasis

289 The first objective of the work was successfully achieved, since indeed the experimental assay
 290 confirmed that **P5** and **P7** can function as HMGC_oAR inhibitors, because both gave statistically
 291 significant concentration-response curves, with calculated IC₅₀ values equal to 147.2 μM for **P5** and
 292 68.4 μM for **P7** (Figure 1). As explained in the introduction, these peptides had been identified in the
 293 basolateral solution of the transport experiments in Caco2 cells by HPLC-chip-ESI-MS/MS and
 294 selected through *in silico* docking simulation experiments as the best candidate for HMGC_oAR
 295 inhibition. In fact, their specific structures favour efficient bindings to the catalytic site of this enzyme
 296 (Lammi, et al., 2016). The peptide-HMGC_oAR complexes appear to be stabilised particularly by the
 297 following interactions: A) The negatively charged residues located at C-terminal tail are engaged in
 298 ionic contacts with Arg568, Arg571, and Lys722; B) The positively charged N-terminus elicits ion-
 299 pairs with Glu559 and Asp767, reinforced by H-bonds with Thr557 and Thr558; C) The hydrophobic
 300 residues located at N-terminus are involved in hydrophobic interactions with apolar residues of
 301 HMGC_oAR. Additionally, **P5** contains a central positively charged residue (Lys5), stabilising a salt
 302 bridge with Asp690. Their activities were postulated to be similar, with a slight preference for **P7**,
 303 since their docking scores, i.e. normalized Plp95, APBS and MPL scores, fell in a very small range
 304 (Lammi, et al., 2016).

305 As indicated in the introduction, in view of better understanding their mode of action, the second
 306 objective was a detailed investigation of their effects on the LDLR pathway in HepG2 cells. To this
 307 scope, **P7** was tested at lower concentrations than **P5**, being a more efficient inhibitor of HMGC_oAR
 308 activity.

309 Our findings clearly suggest that both peptides are able to enhance the protein level of the
 310 transcriptional N-terminal active part of the SREBP2 protein with a statistical significance (Figure
 311 2). In agreement with the increase of active SREBP2 protein, enhancements of the LDLR and
 312 HMGC_oAR protein levels were also detected. to These molecular results are in line with functional
 313 results according to which both **P5** and **P7** are able to increase the HepG2 ability to uptake LDL from
 314 the extracellular environment with a final hypocholesterolemic effect. This last result is in agreement

315 with those published in a recently work in which the treatment with **P5** at a 10 μ M concentration led
316 to an increase of the LDL-uptake by $66\pm 21.4\%$ (Lammi, Zanoni, Aiello, Arnoldi, & Grazioso, 2016).
317 Finally, the results suggest that the activity of **P7** on cholesterol modulation in HepG2 cells is slightly
318 better than that of **P5**.

319 SREBP2 is responsible for the LDLR and HMGC_oAR transcription and SREBP2 maturation is
320 regulated by the intracellular cholesterol homeostasis (Lammi et al., 2014). By inhibiting the
321 HMGC_oAR activity, **P5** and **P7** modulate the intracellular cholesterol biosynthesis and homeostasis,
322 leading to an increase of the LDLR and HMGC_oAR protein levels through the activation of mature
323 SREBP2.

324 In particular, HMGC_oAR is a highly regulated enzyme (Goldstein & Brown, 1990): it can be long-
325 term regulated by the control of its synthesis and its degradation or short-term regulated through
326 phosphorylation or dephosphorylation (Pallottini, Martini, Pascolini, Cavallini, Gori, Bergamini, et
327 al., 2005). The HMGC_oAR transcription and translation increased when the concentrations of the
328 products of the mevalonate pathway are low. Conversely, when the sterol concentrations are high,
329 the intracellular HMGC_oAR concentration decreases (Istvan, Palnitkar, Buchanan, & Deisenhofer,
330 2000). A third level of regulation is achieved through phosphorylation of Ser872 by AMPK, which
331 decreases the enzyme activity (Ching, Davies, & Hardie, 1996). HMGC_oAR is present
332 physiologically in the cell in an active non-phosphorylated form (30%) and an inactive
333 phosphorylated one (70%) (Pallottini et al., 2005).

334 AMPK is expressed in numerous tissues, particularly in the liver, brain and skeletal muscle. Literature
335 reports that some natural compounds, such as policosanols, are able to increase the phosphorylation
336 of AMPK with a direct inhibition of HMGC_oAR (Oliaro-Bosso, Calcio Gaudino, Mantegna, Giraud, Meda,
337 Viola, et al., 2009). Furthermore, it is also known that statins are able to activate AMPK (Sun,
338 Lee, Zhu, Gu, Wang, Zhu, et al., 2006), with the consequence of a synergistic inhibition of
339 HMGC_oAR activity.

340 Our results provide some evidence according to which **P5** and **P7** are able to increase the
341 phosphorylation level of AMPK at the Thr172 residue of the catalytic α subunit, indicating AMPK
342 activation, which in turn produces an inhibition of HMGC_oAR activity (Figure 3). In fact, the AMPK
343 activation mediated by **P5** and **P7** led to a significant increase of the phosphorylation levels of the
344 HMGC_oAR at Ser872 residue, which is the phosphorylation site of AMPK. For this reason, these
345 two peptides are able not only to act as competitive inhibitors of the HMGC_oAR, but also to inhibit
346 HMGC_oAR activity by enhancing AMPK activation (Figure 3). In line with these findings, there is
347 an agreement between the molecular data and *in vitro* results on the **P5** and **P7** ability to interfere
348 with HMGC_oAR activity, since the molecular data shows that they led to an elevation of the p-

349 HMGCoAR/HMGCoAR protein ratio with the consequence of a diminished enzyme activity, as
350 reported in literature (Levy, Ben Djoudi Ouadda, Spahis, Sane, Garofalo, Grenier, et al., 2013). Thus,
351 although **P5** and **P7** determine an increment of HMGCoAR protein levels through SREBP2 activation
352 (Figure 2), the findings clearly suggest that they are also able to negatively regulate the HMGCoAR
353 activity by a direct inhibition of the enzyme catalytic domain (Figure 1) and increase of its
354 phosphorylation through activation of the AMPK pathway (Figure 3), which leads to an increase of
355 p-HMGCoAR/HMGCoAR protein ratio (Figure 4). Other plant peptides share the same mechanism
356 of HMGCoAR inhibition, in particular IAVPGEVA, IAVPTGVA, and LPYP, deriving from soy
357 protein (Lammi, Zanoni, & Arnoldi, 2015).

358 Such detailed studies on the hypocholesterolemic activity of food peptides are very scarce in
359 literature. The first investigated peptide was LRVPAGTTFYVVNPDNDENLRMIA, corresponding
360 to position 301-324 of α' subunit of β -conglycinin (UNIProtKB P11827), a major storage protein of
361 soybean seed belonging to the vicilin-like family. A paper (Lovati, Manzoni, Gianazza, Arnoldi,
362 Kurowska, Carroll, et al., 2000) has demonstrated that it increases the ^{125}I -LDL uptake in human
363 HepG2 cells by 41% and its degradation by 10% *versus* the vehicle at the concentration of 100 μM .
364 Interestingly, absorption experiments conducted in human enterocytes (Amigo-Benavent, Clemente,
365 Caira, Stiuso, Ferranti, & del Castillo, 2014) have shown that YVVNPDNDEN, corresponding to the
366 central sequence of LRVPAGTTFYVVNPDNDENLRMIA, is potentially an absorbed peptide. This
367 prompted a following study (Lammi, Zanoni, Arnoldi, & Vistoli, 2015) showing that it inhibits *in*
368 *vitro* the activity of HMGCoAR with a dose response behaviour and an IC_{50} value equal to 150 μM .
369 Comparing this activity with those of lupin peptides, **P5** is roughly equivalent to YVVNPDNDEN,
370 whereas **P7** appears to be a more efficient inhibitor (Figure 1). *In silico* simulations have shown that
371 also in this case the peptide-HMGCoAR complex is stabilised by the same kind of interactions
372 reported for **P5** and **P7** (Lammi, et al., 2016). Another paper has investigated the effects of
373 YVVNPDNDEN on cholesterol metabolism in HepG2 cells at the concentration of 350 μM (Lammi,
374 Zanoni, Arnoldi, & Vistoli, 2015). YVVNPDNDEN up-regulated the mature SREBP2 protein level
375 by $134.0 \pm 10.5\%$, increased the LDLR protein level by $152.0 \pm 20.0\%$, and enhanced the HMGCoAR
376 protein level by $171 \pm 29.9\%$ *versus* control. Considering the higher concentrations of these
377 experiments, it seems possible to affirm that **P5** and especially **P7** are much more effective than
378 YVVNPDNDEN in regulating cholesterol metabolism.

379 The direct comparison of the functional effects of these peptides on the capability of HepG2 of up-
380 taking extracellular LDL is facilitated by the fact that they were tested all at the same concentration,
381 i.e. 50 μM : again **P7** was the most active, since **P7** increased the LDL uptake by $235.0 \pm 29.2\%$,
382 whereas **P5** produced only $99.5 \pm 48.51\%$ increase (Figure 5), and YVVNPDNDEN by $64.0 \pm 29.9\%$

383 (Lammi, Zanoni, Arnoldi, & Vistoli, 2015). Instead, at the concentration of 10 μ M **P7** and **P5** are
384 almost equivalent.

385 In light with all these data, the conclusions of this experimentation may be summarised in this way:
386 A) both **P5** and **P7** are able to positively modulate the cholesterol metabolism through the inhibition
387 of HMGCoAR activity; B) **P7** is slightly more active than **P5**; C) these lupin peptides are more active
388 than all known soy peptides with which they apparently share the same mechanism of action.

389

390

391 **4.2 Modulation of PCSK9**

392 Proprotein convertase subtilisin/kexin type 9 (PCSK9) has been recently identified as a new target
393 for hypercholesterolemia treatment (Seidah & Prat, 2007). It is an extracellular protein that is
394 expressed primarily in liver, kidney, and intestine (Seidah & Prat, 2012) and plays an important role
395 in regulating hepatic LDLR degradation (Gencer, Lambert, & Mach, 2015; D. W. Zhang, Lagace,
396 Garuti, Zhao, McDonald, Horton, et al., 2007). Notably, since PCSK9 and LDLR are co-regulated by
397 SREBP-2 (Dubuc, Chamberland, Wassef, Davignon, Seidah, Bernier, et al., 2004), increased PCSK9
398 expression in response to statin-induced cellular cholesterol depletion may limit the efficacy of statin
399 treatment (Careskey, Davis, Alborn, Troutt, Cao, & Konrad, 2008; Welder, Zineh, Pacanowski,
400 Troutt, Cao, & Konrad, 2010). The development of therapies that inhibit PCSK9 function holds
401 promise for improved management of hypercholesterolemia and cardiovascular disease risk.
402 Particularly, some evidence supports the direct binding of secreted PCSK9 to LDLR, resulting in
403 receptor degradation (Cameron, Holla, Ranheim, Kulseth, Berge, & Leren, 2006; Lagace, Curtis,
404 Garuti, McNutt, Park, Prather, et al., 2006). The PCSK9 binding site in the LDLR is located at the
405 first epidermal growth factor-like repeat (EGF-A) of the extracellular domain (Zhang, et al., 2007)
406 and this protein-protein interaction (PPI) is necessary for LDLR degradation.

407 The idea of investigating PCSK9 modulation in this case was stimulated by recent literature. A
408 clinical study has demonstrated that consuming dietary bars containing 30 g lupin protein per day
409 changed the plasma levels of PCSK9 by -8.5% ($p = 0.0454$) *versus* the control group (casein bar) in
410 mild hypercholesterolemic subjects (Lammi, Zanoni, Calabresi, & Arnoldi, 2016). In addition, peptic
411 and tryptic hydrolysates from lupin protein positively influenced intracellular PCSK9 processing in
412 hepatocytes (Lammi, Zanoni, Calabresi, & Arnoldi, 2016) and the basolateral samples from the
413 absorption experiments on Caco-2 cells were able to interfere with the PCSK9/LDLR PPI (Lammi,
414 Zanoni, Aiello, Arnoldi, & Grazioso, 2016). This activity may be primarily attributable to **P5**, which
415 was demonstrated to be a potent inhibitor of the interaction of PCSK9 with the LDLR, with a very
416 low IC_{50} value equal to 1.6 μ M. In particular, we have demonstrated that **P5** is able to impair the

417 interaction of PCSK9 with the LDLR in a dose-dependent manner using a PCSK9-LDLR *in vitro*
418 binding assay (Lammi, Zanoni, Aiello, Arnoldi, & Grazioso, 2016). It is useful to observe that Pep2-
419 8 (Ac-TVFTSWEEYLDWV-amide), the best inhibitor of this PPI singled out in a recent paper (
420 Zhang, Eigenbrot, Zhou, Shia, Li, Quan, et al., 2014), has an IC₅₀ value equal of $0.81 \pm 0.08 \mu\text{M}$, i.e.
421 only slightly better than that of **P5**. Interestingly, Pep2-8 contains 13 amino acid residues and its C-
422 terminal truncated analogues lose activity, whereas **P5** contains only 10 residues. **P5** is thus one of
423 the shortest peptides ever described in literature endowed with this specific activity.

424 This stimulated us to investigate whether **P5** as well as **P7** are able to modulate PCSK9 intracellular
425 processing. Indeed, **P5** induced a reduction of mature PCSK9 protein level and a consequent decrease
426 of mature PCSK9 secretion. In order to elucidate the mechanism through which this peptide positively
427 affect the LDLR pathway by reducing the PCSK9 protein level and secretion, a crucial aspect is the
428 regulation of PCSK9 transcription. Several transcription factors, such as SREBPs and HNF-1, have
429 been identified as transcriptional activators of PCSK9 gene expression (Horton, Shah, Warrington,
430 Anderson, Park, Brown, et al., 2003; Li, Dong, Park, Lee, Chen, & Liu, 2009). PCSK9 and LDLR
431 both contain functional sterol regulatory elements (SREs) in their promoters that respond to change
432 in intracellular cholesterol levels through the activation of the SREBP pathway (Dubuc, et al., 2004;
433 Maxwell, Soccio, Duncan, Sehayek, & Breslow, 2003). However, since the HNF1-alpha binding site
434 is unique to the PCSK9 promoter and is not present in the LDLR promoter, modulation of PCSK9
435 transcription through HNF1-alpha sequence does not affect LDLR gene expression. Thus, the HNF1-
436 alpha binding site represents a divergent point to disconnect the co-regulation of PCSK9 from LDLR
437 and other SREBP target genes (Dong, Li, Singh, Cao, & Liu, 2015). Interestingly, we have shown
438 here that only **P5** decreased hepatic PCSK9 production (Figure 6 A,C) and extra cellular secretion
439 (Table 1), without increasing LDLR protein levels and other SREBP-2 target genes (such as
440 HMGCoAR), and down-regulates HNF1-alpha protein content in HepG2 cells (Figure 6 A,C).

441 The behaviour of **P7** instead is quite different, since it increased the intracellular LDLR protein levels
442 through activation of SREBP2 leading to an increased ability of HepG2 cells to uptake extracellular
443 LDL, without affecting PCSK9 and HNF1-alpha protein levels (Figure 6 B-D).

444 In conclusion, we have identified in lupin protein hydrolysates **P5** and **P7**, two peptides that share the
445 capacity to up-regulate the LDLR-SREBP2 pathway, leading to an improved HepG2 capability to
446 uptake LDL, but greatly diverge in the modulation of intracellular PCSK9 processing and
447 extracellular excretion where only **P5** is active. The molecular mechanisms of these peptides may in
448 part explain the hypocholesterolemic activity observed in clinical trials et al., 2015; Lammi, Zanoni,
449 Calabresi, & Arnoldi, 2016; Sirtori, et al., 2012) and in animal studies (Betzliche, Brandsch,
450 Schmidt, Weisse, Eder, & Stangl, 2008; Marchesi, Parolini, Diani, Rigamonti, Cornelli, Arnoldi, et

451 al., 2008; Parolini, Rigamonti, Marchesi, Busnelli, Cinquanta, Manzini, et al., 2012; Sirtori, Lovati,
452 Manzoni, Castiglioni, Duranti, Magni, et al., 2004).

453

454 **AUTHORS CONTRIBUTIONS**

455 Experiment ideation and design: CL. Experiments & data analysis: biological experiments CL & CZ;
456 peptide identification and analysis GA. Figure preparation: CZ. Grant retrieval: AA. Manuscript
457 writing: CL & AA.

458

459 **ACKNOWLEDGMENTS**

460 We are indebted to Carlo Sirtori Foundation (Milan, Italy) for having provided part of equipment
461 used in this experimentation.

462

463 **SOURCES OF FUNDING**

464 Researches funded in part by the European Union Seventh Framework Programme (FP7/2007–2013),
465 under grant agreement no. 285819.

466

467

468 **REFERENCES**

- 469 Amigo-Benavent, M., Clemente, A., Caira, S., Stiuso, P., Ferranti, P., & del Castillo, M. D. (2014).
470 Use of phytochemomics to evaluate the bioavailability and bioactivity of antioxidant peptides
471 of soybean β -conglycinin. *Electrophoresis*, 35(11), 1582-1589.
- 472 Arnoldi, A., Boschin, G., Zanoni, C., & Lammi, C. (2015). The health benefits of sweet lupin seed
473 flours and isolated proteins. *Journal of Functional Foods*, 18, 550-563.
- 474 Bettzieche, A., Brandsch, C., Schmidt, M., Weisse, K., Eder, K., & Stangl, G. (2008). Differing effect
475 of protein isolates from different cultivars of blue lupin on plasma lipoproteins of
476 hypercholesterolemic rats. *Bioscience, Biotechnology, and Biochemistry*, 72(12), 3114-3121.
- 477 Bähr, M., Fechner, A., Kiehntopf, M., & Jahreis, G. (2015). Consuming a mixed diet enriched with
478 lupin protein beneficially affects plasma lipids in hypercholesterolemic subjects: a
479 randomized controlled trial. *Clinical Nutrition*, 34(1), 7-14.
- 480 Cameron, J., Holla, Ø., Ranheim, T., Kulseth, M. A., Berge, K. E., & Leren, T. P. (2006). Effect of
481 mutations in the PCSK9 gene on the cell surface LDL receptors. *Human Molecular Genetics*,
482 15(9), 1551-1558.
- 483 Careskey, H. E., Davis, R. A., Alborn, W. E., Troutt, J. S., Cao, G., & Konrad, R. J. (2008).
484 Atorvastatin increases human serum levels of proprotein convertase subtilisin/kexin type 9.
485 *Journal of Lipid Research*, 49(2), 394-398.
- 486 Ching, Y. P., Davies, S. P., & Hardie, D. G. (1996). Analysis of the specificity of the AMP-activated
487 protein kinase by site-directed mutagenesis of bacterially expressed 3-hydroxy 3-
488 methylglutaryl-CoA reductase, using a single primer variant of the unique-site-elimination
489 method. *European Journal of Biochemistry*, 237(3), 800-808.
- 490 Dong, B., Li, H., Singh, A. B., Cao, A., & Liu, J. (2015). Inhibition of PCSK9 transcription by
491 berberine involves down-regulation of hepatic HNF1 α protein through the ubiquitin-
492 proteasome degradation pathway. *Journal of Biological Chemistry*, 290(7), 4047-4058.
- 493 Dubuc, G., Chamberland, A., Wassef, H., Davignon, J., Seidah, N. G., Bernier, L., & Prat, A. (2004).
494 Statins upregulate PCSK9, the gene encoding the proprotein convertase neural apoptosis-
495 regulated convertase-1 implicated in familial hypercholesterolemia. *Arteriosclerosis
496 Thrombosis and Vascular Biology*, 24(8), 1454-1459.

- 497 Duranti, M., Consonni, A., Magni, C., Sessa, F., & Scarafoni, A. (2008). The major proteins of lupin
498 seed: characterisation and molecular properties for use as functional and nutraceutical
499 ingredients. *Trends in Food Science and Technology*, *19*(12), 624-633.
- 500 Ferruzza, S., Rossi, C., Scarino, M. L., & Sambuy, Y. (2012). A protocol for differentiation of human
501 intestinal Caco-2 cells in asymmetric serum-containing medium. *Toxicology In Vitro*, *26*(8),
502 1252-1255.
- 503 Gencer, B., Lambert, G., & Mach, F. (2015). PCSK9 inhibitors. *Swiss Medicine Weekly*, *145*,
504 w14094.
- 505 Goldstein, J. L., & Brown, M. S. (1990). Regulation of the mevalonate pathway. *Nature*, *343*(6257),
506 425-430.
- 507 Horton, J. D., Shah, N. A., Warrington, J. A., Anderson, N. N., Park, S. W., Brown, M. S., &
508 Goldstein, J. L. (2003). Combined analysis of oligonucleotide microarray data from
509 transgenic and knockout mice identifies direct SREBP target genes. *Proceedings of the*
510 *National Academy of Sciences of the United States of America*, *100*(21), 12027-12032.
- 511 Istvan, E. S., Palnitkar, M., Buchanan, S. K., & Deisenhofer, J. (2000). Crystal structure of the
512 catalytic portion of human HMG-CoA reductase: insights into regulation of activity and
513 catalysis. *Embo Journal*, *19*(5), 819-830.
- 514 Lagace, T. A., Curtis, D. E., Garuti, R., McNutt, M. C., Park, S. W., Prather, H. B., Anderson, N. N.,
515 Ho, Y. K., Hammer, R. E., & Horton, J. D. (2006). Secreted PCSK9 decreases the number of
516 LDL receptors in hepatocytes and in livers of parabiotic mice. *J of Clinica Investigation*,
517 *116*(11), 2995-3005.
- 518 Lammi, C., Aiello, G., Vistoli, G., Zanoni, C., Arnoldi, A., Sambuy, Y., Ferruzza, S., & Ranaldi, G.
519 (2016). A multidisciplinary investigation on the bioavailability and activity of peptides from
520 lupin protein. *Journal of Functional Foods*, *24*, 297-306.
- 521 Lammi, C., Zanoni, C., Aiello, G., Arnoldi, A., & Grazioso, G. (2016). Lupin Peptides Modulate the
522 Protein-Protein Interaction of PCSK9 with the Low Density Lipoprotein Receptor in HepG2
523 Cells. *Scientific Reports*, *6*.
- 524 Lammi, C., Zanoni, C., & Arnoldi, A. (2015). IAVPGEVA, IAVPTGVA, and LPYP, three peptides
525 from soy glycinin, modulate cholesterol metabolism in HepG2 cells through the activation of
526 the LDLR-SREBP2 pathway. *Journal of Functional Foods*, *14*, 469-478.

- 527 Lammi, C., Zanoni, C., Arnoldi, A., & Vistoli, G. (2015). Two peptides from soy beta-conglycinin
528 induce a hypocholesterolemic effect in HepG2 cells by a statin-Like mechanism: comparative
529 in vitro and in silico modeling studies. *Journal of Agricultural and Food Chemistry*, 63(36),
530 7945-7951.
- 531 Lammi, C., Zanoni, C., Calabresi, L., & Arnoldi, A. (2016). Lupin protein exerts cholesterol-lowering
532 effects targeting PCSK9: From clinical evidences to elucidation of the in vitro molecular
533 mechanism using HepG2 cells. *Journal of Functional Foods*, 23, 230-240.
- 534 Lammi, C., Zanoni, C., Ferruzza, S., Ranaldi, G., Sambuy, Y., & Arnoldi, A. (2016).
535 Hypocholesterolaemic Activity of Lupin Peptides: Investigation on the Crosstalk between
536 Human Enterocytes and Hepatocytes Using a Co-Culture System Including Caco-2 and
537 HepG2 Cells. *Nutrients*, 8(7).
- 538 Lammi, C., Zanoni, C., Scigliuolo, G. M., D'Amato, A., & Arnoldi, A. (2014). Lupin peptides lower
539 low-density lipoprotein (LDL) cholesterol through an up-regulation of the LDL
540 receptor/sterol regulatory element binding protein 2 (SREBP2) pathway at HepG2 cell line.
541 *Journal of Agricultural and Food Chemistry*, 62(29), 7151-7159.
- 542 Levy, E., Ben Djoudi Ouadda, A., Spahis, S., Sane, A. T., Garofalo, C., Grenier, É., Emonnot, L.,
543 Yara, S., Couture, P., Beaulieu, J. F., Ménard, D., Seidah, N. G., & Elchebly, M. (2013).
544 PCSK9 plays a significant role in cholesterol homeostasis and lipid transport in intestinal
545 epithelial cells. *Atherosclerosis*, 227(2), 297-306.
- 546 Li, H., Dong, B., Park, S. W., Lee, H. S., Chen, W., & Liu, J. (2009). Hepatocyte nuclear factor 1alpha
547 plays a critical role in PCSK9 gene transcription and regulation by the natural
548 hypocholesterolemic compound berberine. *Journal of Biological Chemistry*, 284(42), 28885-
549 28895.
- 550 Lovati, M. R., Manzoni, C., Gianazza, E., Arnoldi, A., Kurowska, E., Carroll, K. K., & Sirtori, C. R.
551 (2000). Soy protein peptides regulate cholesterol homeostasis in Hep G2 cells. *Journal of*
552 *Nutrition*, 130(10), 2543-2549.
- 553 Marchesi, M., Parolini, C., Diani, E., Rigamonti, E., Cornelli, L., Arnoldi, A., Sirtori, C. R., & Chiesa,
554 G. (2008). Hypolipidaemic and anti-atherosclerotic effects of lupin proteins in a rabbit model.
555 *British Journal of Nutrition*, 100(4), 707-710.
- 556 Maxwell, K. N., Soccio, R. E., Duncan, E. M., Sehayek, E., & Breslow, J. L. (2003). Novel putative
557 SREBP and LXR target genes identified by microarray analysis in liver of cholesterol-fed
558 mice. *Journal of Lipid Research*, 44(11), 2109-2119.

- 559 Oliaro-Bosso, S., Calcio Gaudino, E., Mantegna, S., Giraud, E., Meda, C., Viola, F., & Cravotto, G.
560 (2009). Regulation of HMGCoA reductase activity by policosanol and octacosadienol, a new
561 synthetic analogue of octacosanol. *Lipids*, *44*(10), 907-916.
- 562 Pallottini, V., Martini, C., Pascolini, A., Cavallini, G., Gori, Z., Bergamini, E., Incerpi, S., &
563 Trentalance, A. (2005). 3-Hydroxy-3-methylglutaryl coenzyme A reductase deregulation and
564 age-related hypercholesterolemia: A new role for ROS. *Mechanisms of Ageing and*
565 *Development*, *126*(8), 845-851.
- 566 Parolini, C., Rigamonti, E., Marchesi, M., Busnelli, M., Cinquanta, P., Manzini, S., Sirtori, C., &
567 Chiesa, G. (2012). Cholesterol-lowering effect of dietary *Lupinus angustifolius* proteins in
568 adult rats through regulation of genes involved in cholesterol homeostasis. *Food Chemistry*,
569 *132*(3), 1475-1479.
- 570 Sambuy, Y., De Angelis, I., Ranaldi, G., Scarino, M. L., Stamatii, A., & Zucco, F. (2005). The Caco-
571 2 cell line as a model of the intestinal barrier: influence of cell and culture-related factors on
572 Caco-2 cell functional characteristics. *Cell Biology and Toxicology*, *21*(1), 1-26.
- 573 Seidah, N. G., & Prat, A. (2007). The proprotein convertases are potential targets in the treatment of
574 dyslipidemia. *Journal of Molecular Medicine (Berlin)*, *85*(7), 685-696.
- 575 Seidah, N. G., & Prat, A. (2012). The biology and therapeutic targeting of the proprotein convertases.
576 *Nature reviews. Drug discovery*, *11*(5), 367-383.
- 577 Sirtori, C. R., Lovati, M. R., Manzoni, C., Castiglioni, S., Duranti, M., Magni, C., Morandi, S.,
578 D'Agostina, A., & Arnoldi, A. (2004). Proteins of white lupin seed, a naturally isoflavone-
579 poor legume, reduce cholesterolemia in rats and increase LDL receptor activity in HepG2
580 cells. *Journal of Nutrition*, *134*(1), 18-23.
- 581 Sirtori, C. R., Triolo, M., Bosisio, R., Bondioli, A., Calabresi, L., De Vergori, V., Gomaschi, M.,
582 Mombelli, G., Pazzucconi, F., Zacherl, C., & Arnoldi, A. (2012). Hypocholesterolaemic
583 effects of lupin protein and pea protein/fibre combinations in moderately
584 hypercholesterolaemic individuals. *British Journal of Nutrition*, *107*(8), 1176-1183.
- 585 Sun, W., Lee, T. S., Zhu, M., Gu, C., Wang, Y., Zhu, Y., & Shyy, J. Y. (2006). Statins activate AMP-
586 activated protein kinase in vitro and in vivo. *Circulation*, *114*(24), 2655-2662.
- 587 Welder, G., Zineh, I., Pacanowski, M. A., Troutt, J. S., Cao, G., & Konrad, R. J. (2010). High-dose
588 atorvastatin causes a rapid sustained increase in human serum PCSK9 and disrupts its
589 correlation with LDL cholesterol. *Journal of Lipid Research*, *51*(9), 2714-2721.

- 590 Zhang, D. W., Lagace, T. A., Garuti, R., Zhao, Z., McDonald, M., Horton, J. D., Cohen, J. C., &
591 Hobbs, H. H. (2007). Binding of proprotein convertase subtilisin/kexin type 9 to epidermal
592 growth factor-like repeat A of low density lipoprotein receptor decreases receptor recycling
593 and increases degradation. *Journal of Biological Chemistry*, 282(25), 18602-18612.
- 594 Zhang, Y., Eigenbrot, C., Zhou, L., Shia, S., Li, W., Quan, C., Tom, J., Moran, P., Di Lello, P.,
595 Skelton, N. J., Kong-Beltran, M., Peterson, A., & Kirchhofer, D. (2014). Identification of a
596 small peptide that inhibits PCSK9 protein binding to the low density lipoprotein receptor.
597 *Journal of Biological Chemistry*, 289(2), 942-955.
- 598